

2018

Effect of Hydrogen on Pristine Amorphous V2O5 Thin Film

H. H. Afify

Physics Sector, Solid State Physics Department, National Research Center, Dokki, Cairo, Egypt,
moh_al90@yahoo.com

M. E. Hassan

Physics Department, Aswan University, Aswan, Egypt, moh_al90@yahoo.com

A. M. Badr

Physics Department, Aswan University, Aswan, Egypt, moh_al90@yahoo.com

H. A. Elsheikh

Physics Department, Aswan University, Aswan, Egypt, moh_al90@yahoo.com

Follow this and additional works at: <https://digitalcommons.aaru.edu.eg/ijtfst>

Recommended Citation

H. Afify, H.; E. Hassan, M.; M. Badr, A.; and A. Elsheikh, H. (2018) "Effect of Hydrogen on Pristine Amorphous V2O5 Thin Film," *International Journal of Thin Film Science and Technology*: Vol. 7 : Iss. 1 , Article 1.

Available at: <https://digitalcommons.aaru.edu.eg/ijtfst/vol7/iss1/1>

This Article is brought to you for free and open access by Arab Journals Platform. It has been accepted for inclusion in International Journal of Thin Film Science and Technology by an authorized editor. The journal is hosted on [Digital Commons](#), an Elsevier platform. For more information, please contact rakan@aarj.edu.eg, marah@aarj.edu.eg, u.murad@aarj.edu.eg.

Effect of Hydrogen on Pristine Amorphous V_2O_5 Thin Film

H. H. Afify¹, M. E. Hassan^{2*}, A. M. Badr² and H. A. Elsheikh²

1 Physics Sector, Solid State Physics Department, National Research Center, Dokki, Cairo, Egypt,

2 Physics Department Aswan University Aswan Egypt

Received: 28 Sep. 2017, Revised: 1 Dec. 2017, Accepted: 5 Dec. 2017.

Published online: 1 Jan. 2018.

Abstract: Sequentially deposited layer by layer up to five vanadium oxide film is deposited on glass and silica substrates at 300 k by vacuum thermal evaporation technique. The deposited samples subjected to reduction process in the preparation site by hydrogen gas at 473k for 10 minutes and 573 k for 10, 20 minutes. The XRD investigation of the samples demonstrates that the pristine sample is amorphous while those reduced are crystalline. The existed phases in virgin samples are educated by Raman spectroscopy which indicates the single V_2O_5 phase. The different phases in the reduced sample are identified by analyzing their XRD patterns. The electrical resistance of the reduced samples is measured as a function of temperature during heating and cooling cycles. The transition temperature from semiconducting to metal state is defined by the derivative of dR/dT .

Keywords: Smart window; thermochromics martial; Vanadium dioxide; mlti-layers.

1 Introduction

Vanadium oxides (VO_x) have attracted more attention because of their capability of going through a reversible metal-insulator transition (MIT), during which the electrical conductivity can change by several orders of magnitude [1]. This remarkable and reversible transition makes them of considerable technological interests. For example, VO_2 undergoes an MIT at 68 °C, along with a dramatic change in its optical properties in the near infrared band, making it highly suitable for applications such as optoelectronics, ultra-fast optical switches, and smart windows [2–4]. V_2O_3 and V_2O_5 have been widely used as catalysts in gas sensors, lithium ion battery as well as a variety of industrial processes [5–7]. V_2O_5 can also be found in electrochromic devices as electrochromic layers [8]. However, it remains a great challenge to deposit VO_x thin films with single stoichiometry. First, this is because the vanadium-oxygen system is highly complicated due to the multivalency of vanadium. In phase diagram, there are nearly twenty stable VO_x phases, such as VO, V_2O_3 , V_4O_7 , VO_2 , V_3O_5 , and V_2O_5 , while each VO_x is stable only within a narrow window [9]. Second, structural characterization of VO_x of different stoichiometry is complicated and incomplete due to its complex valence states. However, X-ray diffraction (XRD) is not highly sensitive and cannot identify minor amount of impurity

phases [10]. Relatively, Raman spectroscopy is a more powerful structure characterization technique for VO_x because of its high sensitivity. However, the interpretation of Raman spectra relies on comparing the measured spectra with reference spectra and available Raman data for VO_x are limited and in some cases unclear [12, 13]. Those obstacles in structural characterization of VO_x add difficulties to the synthesis of VO_x thin films with single stoichiometry. VO_x thin films with unidentified impurity phases usually lead to unexpected poor performance in applications. In this research, VO_x thin films with different stoichiometry under various bonding states are successfully prepared by thermal evaporation with and without post reduction. The samples were then characterized using Raman spectroscopy and thus the phase evolution could be clarified. The results presented would facilitate both vanadium oxide materials preparation and their structural characterization.

2 Experimental procedures

Thin films of V_2O_5 have been deposited by thermal evaporation in a vacuum deposition chamber on top of Corning glass and silica substrates. The source material (99.5% pure V_2O_5 powder RIEDEL- HAEN Ag SEELZE-HANNOVER) has been evaporated from a Molybdenum boat. The deposition pressure in the chamber has been maintained between 4×10^{-6} and 9×10^{-6} mbar and the source–substrate distance has been kept at approximately

*Corresponding author E-mail: moh_al90@yahoo.com

25cm. The thermal evaporation, and post reduction has been performed using furnace (Edward 306A PVD) with a ramp up of 15 K/min and a holding time of 10 min , varying the temperature between 200 °C and 300 °C (with steps of 10/min), under low pressure 10^{-3} milibar in hydrogen gas conditions. In order to control the effect of post-reduction temperature, each deposition has been performed over a batch of ten substrates from which seven samples were selected for post-reduction. The thicknesses of the films and each layer are measured by quartz crystal monitor built in the evaporation system. The structural properties of the deposited films have been diagnosed by X-ray diffractometer, Shimadzu XRD-6000, with Cu radiation $\lambda=1.54056$ Å. The X-ray tube was operated at 40 kV and 30 mA anode current throughout the measurements. XRD patterns were collected with a scanning step of 0.02° over the angular 2θ range $10-90^\circ$, with a total acquisition time of 15 min. The surface microstructural properties have been analyzed using scanning electron microscopy with (HRSEM) – Quanta-FEG250 system, and manufactured by Bruker. Model: MLCT-MT-A.

Atomic force microscopy has been performed contact mode using nonconductive silicon nitride probe, top coated with Al and choosing the resolution of the image as 512 lines by 512 columns with a scan size of 256×256 data points. The electrical conductivity versus temperature has been measured in samples homemade measurement system. Critical Temperature has been determined by differentiation of the thermoresistance hysteresis.

3. Results and discussion

3.1 Phase identification

The XRD patterns for the investigated samples are shown in Fig.1 It is clear the as deposited sample shows only a broad hump in 2θ 15 to 35 range which mainly related to the amorphous glass substrate. Therefore the deposited material is amorphous. In order to identify the as deposited amorphous sample it is subjected to Raman spectroscopy to determine the existed phase. The obtained spectrum is shown in fig.1 Six clear Raman bands are observed at 144,285,409,506,688,and 991 cm^{-1} . These peaks are to great extent matched well with that reported and assigned to the vibration bands of the as deposited amorphous V_2O_5 [10,12,15].

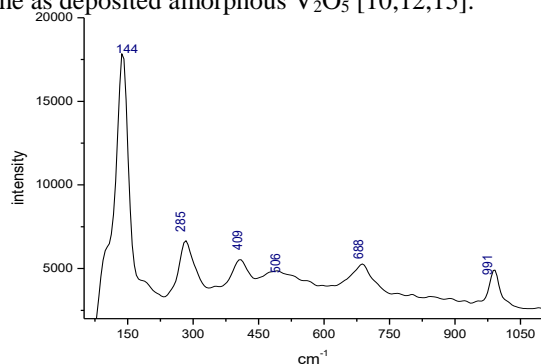


Fig 1 Raman spectra for five layers deposition virain sample

When the sample is exposed to Hydrogen gas with constant flow rate and different times at 200 °C & 300 °C the samples show a clear and well defined XRD patterns. This means that the as deposited sample changes from amorphous nature to crystalline one by heat treatment under hydrogen gas. The detailed information about the crystalline structure of the sample at each heat treatment condition will be obtained by analysis of their XRD patterns. The sample heated at 200 °C and constant flow rate of Hydrogen gas for 10 minutes shows two distinct monoclinic VO_2 & α , and γ V_2O_5 phases. The XRD Pattern of this sample given in Fig.2 Shows reasonable intensity reflection in the (100),(011),(110) planes (at $2\theta = 9.62^\circ, 13.96^\circ, 26.62^\circ$) respectively , which corresponds to a monoclinic VO_2 phase (JCPDS71#-0290) [12]. Also additional reflections that correspond to V_2O_5 growth (at $2\theta = 18.66^\circ, 29.26^\circ, 31^\circ$) [15] are observed. The XRD pattern for samples heated at 300 °C and exposed to hydrogen with the same flow rate for 10 min indicates nearly complete disappearance of V_2O_5 phase and emerges of V_4O_7 phase demonstrated by only the appearance of (100) as indexed by JCPDS# fil 18-1452. Meanwhile the reflection planes (100), (011) & (110) which corresponds to VO_2 phase still exists. When the hydrogen exposure time is increased to 20 minutes the V_4O_7 phase is vanished while the peaks related to VO_2 stay with slight increase in their intensity and are strong existence and appearance of V_3O_5 displayed as: (2 0 2) at 38.57° , (002) at 44.78° , (224) at $64.91^\circ, 78.2^\circ$ Indicated by (JCPDS# 72-0977) standard card, with lattice parameter ($a=9.859, b=5.0416, c=6.991$). This means that the sample heated at 300 °C and exposed to hydrogen gas with constant flow rate for 20 minutes exhibits only $\text{VO}_2, \text{V}_3\text{O}_5$ phases while those heated at 200 °C & 300 °C for 10 minutes show $\text{VO}_2, \text{V}_4\text{O}_7, \text{V}_2\text{O}_5$ phases.

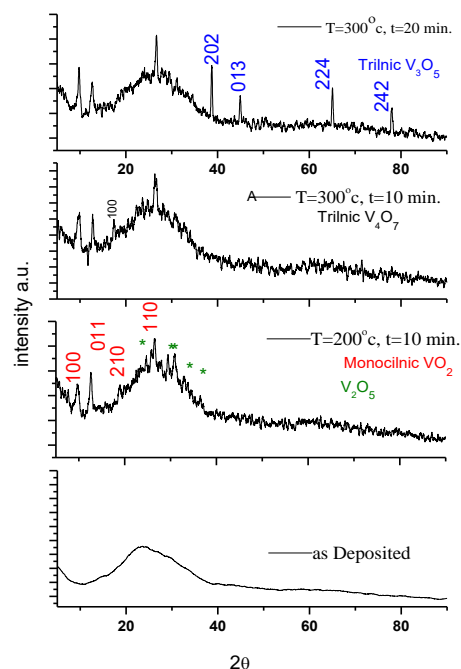


Fig (2) XRD as deposited, reduced at $T=200^\circ\text{C}, 300^\circ\text{C}$ for 10 min., and 300°C for 20 min

3.2 Electrical measurements

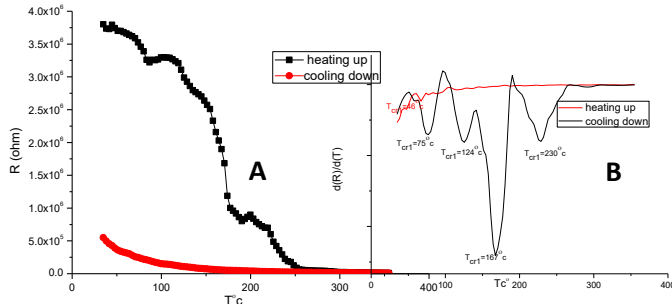


Fig (3) Reduction temperature $T=200\text{ }^{\circ}\text{C}$ for 10min A electrical resistance, B differentiate of electrical resistance

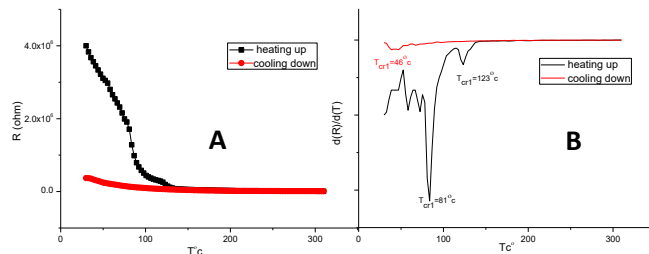


Fig (4) Reduction temperature $T=300\text{ }^{\circ}\text{C}$ for 10 min A electrical resistance, B differentiate of electrical resistance

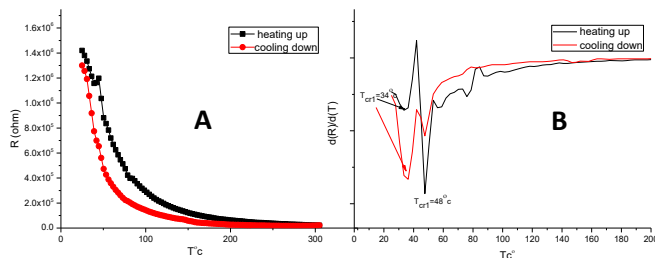


Fig (5) Reduction temperature $T=300\text{ }^{\circ}\text{C}$ for 20 min A electrical resistance, B differentiate of electrical resistance via temperature

The variation of the electrical resistance (R) of the films with different reduction time and temperature as a function of temperature (T) during the heating up and cooling down processes are shown in Fig. 2, 5, 4. A sharp decrease in resistance of the sample reduced at $200\text{ }^{\circ}\text{C}$ (in Fig. 4-A) are observed at temperatures in the vicinity of $157\text{ }^{\circ}\text{C}$ during the heating. This result shows that two orders of magnitude change occurs in resistance during thermal cycling, which is due to the semiconductor-metal (S-M) transition of the vanadium oxide film. In order to clarify the switching behavior of resistance accurately, the derivative of the resistance for the heating process was calculated by $(d(R))/dT$, The obtained result is shown in Fig 3-B. The transition temperature (T_{cr}) is defined as the center of the derivative curve and the minimum bottom is given to describe the abruptness or sharpness of the transition temperature as indicated in Fig (3-B), the T_{cr} of the reduced film at $200\text{ }^{\circ}\text{C}$ for 10 min is $157\text{ }^{\circ}\text{C}$. When the reduction temperature increases from 200 to $300\text{ }^{\circ}\text{C}$, the T_{cr} diminishes from 157 to $81\text{ }^{\circ}\text{C}$.

The high transition temperature value for samples reduced at $200\text{ }^{\circ}\text{C}$ may be attributed to the incomplete reduction and the existence of nonstoichiometric phases such as $[\text{V}_2\text{O}_5, \text{VO}_2]$. Also, the weak intensity of XRD reflects the small grain size of the formed phases which allow an increase in the transition temperature. It is reported that the S-M transition temperature of VO_2 film is about $68\text{ }^{\circ}\text{C}$ [5] and that of V_2O_5 film is $257\text{ }^{\circ}\text{C}$ [15]. Youn et al. Found that the T_{cr} of vanadium oxide increases as VO_2 changes to V_2O_5 [16]. Wei et al. presented that the grain size and crystallization of vanadium oxide film will influence the T_{cr} [17]. Therefore, the little amount of VO_2 and other phases with low crystallization state in the investigated samples will reduce the transition temperature for values lower than $250\text{ }^{\circ}\text{C}$ corresponding V_2O_5 and higher than that for VO_2 ($68\text{ }^{\circ}\text{C}$). In addition, as shown in Fig. 2, the width of hysteresis is defined as the difference between the transition temperatures of heating and cooling processes of the hysteresis loop. It is found that when the film reduced temperature increases from 200 to $300\text{ }^{\circ}\text{C}$, and reduction time increase from 10 to 20 min, the hysteresis loop width decreases from 150 to $40\text{ }^{\circ}\text{C}$. This result demonstrates that the T_{cr} depends on the film Reduction time and temperature. It is obvious that samples subjected to reduction at higher temperature and longer dwelling time exhibit lower transition temperature. Therefore, samples reduced at $300\text{ }^{\circ}\text{C}$ for 20 minutes show lower values of transition ($48\text{ }^{\circ}\text{C}$) while these reduced at $300\text{ }^{\circ}\text{C}$ for 10 minutes shows higher value of transition temperature ($81\text{ }^{\circ}\text{C}$). This reduction in transition temperature could be due to reduction of the pristine V_2O_5 followed by emerge and evolution of VO_2 and the other reduced phases such as V_4O_7 & V_3O_5 . The obtained results are, to great extent, in good agreement with that reported in literature. [5,8,9].

3.3 Scanning electron microscopy and atomic force microscopy

Surface microstructures obtained through HRSEM analysis (top view) are depicted in Fig. 5, 6, and 7 show the effect of post reduction temperature, and time. The SEM images are complemented by AFM analysis (height and phase channels) performed over the same samples, which are shown in Fig. 8, 9,10 and 11 respectively. When the thin films are reduced at $T = 200\text{ }^{\circ}\text{C}$ we observe V_2O_5 crystals distended in rod like shape disposed in stacked layers, Fig. 5. Further increase in T up to $300\text{ }^{\circ}\text{C}$ for 10 min, and 20 min led to the enlargement of crystallites as evidenced in Fig. 6,7 and the grains growth in different directions, as supported by the XRD data.

Fig. 5, 6 and f shows the morphology on a $2 \times 2\text{ }\mu\text{m}^2$ surface area of V_2O_5 and to further detect the microstructure, and nanostructure of the composite film, high resolution scanning electron microscopy (HRSEM). As shown in Fig. 5, the compositions of Nano rod with length of 20 micrometer with diameter 150 nm with primary composed of Nano- sphere at reduction temperature $T=200\text{ }^{\circ}\text{C}$ for 10 min, Fig. 6 Micrographs of the film indicate that crystallites are well formed with the increasing of Reduction temperature up to $300\text{ }^{\circ}\text{C}$ for 10 min gives smooth surface. From these micrographs, the distribution of grain sizes of

VO₂, V₃O₅ film deposited has been oriented and composed as Nano sphere like with average diameter 95 nm measured. By increasing reduction time up to 20 min. at reduction temperature T=300°C the compositions of high homogenously fine structure of Nano sphere like at fig 7 with the decreasing of diameter of Nano sphere up to 50 nm. [9, 8].

the mean square and average roughness of the film surfaces and the mean diameter of the grains (Fig10, 11). The roughness decreases lightly as the reduction temperature increase look table(1), also the particle size and grains decrease from 60 nm at reduction temperature 200°C for 10 min to 45 nm with the increasing of reduction temperature up to 300°C as it is in fig(10, 11) [10,11,12].

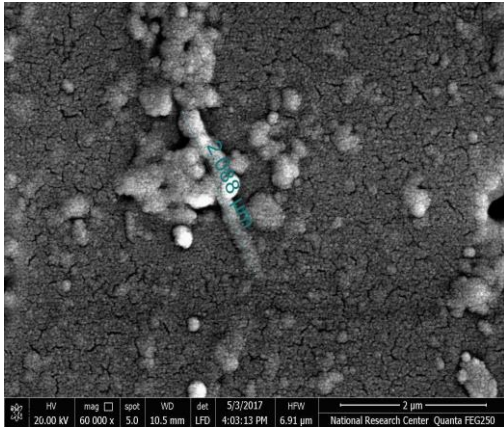


Fig (6) Reduction temperature T=200 °c for 10 min High resolution Scanning Electron microscope (HRSEM)

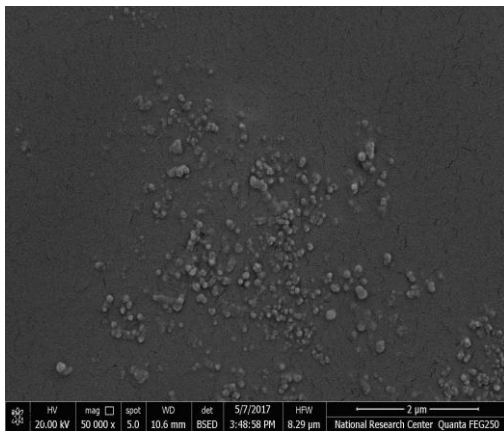


Fig (7) Reduction temperature T=300 °c for 10 min High resolution Scanning Electron microscope (HRSEM)

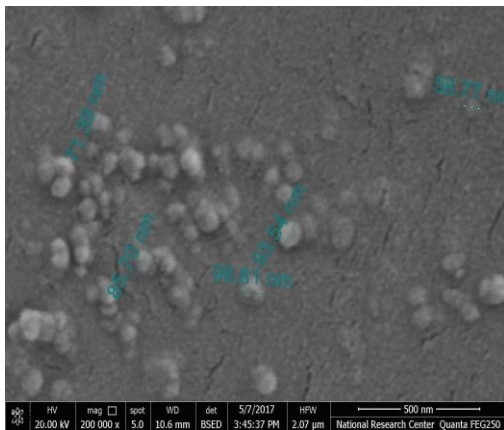


Fig (8) High resolution Scanning Electron microscope (HRSEM) at reduction Temperature 300°C for 20 min

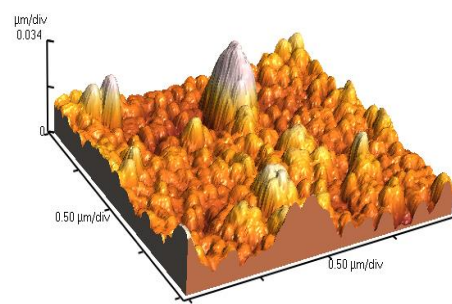


Fig (9) Reduction temperature T=200 °c for 10 min Atomic Force Microscope (AFM)

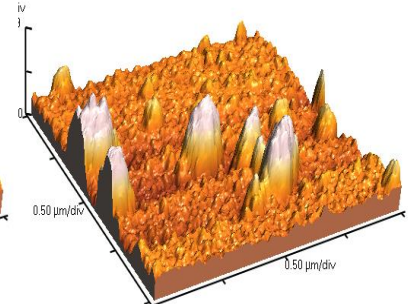


Fig (10) Reduction temperature T=300 °c for 10 min Atomic Force Microscope (AFM)

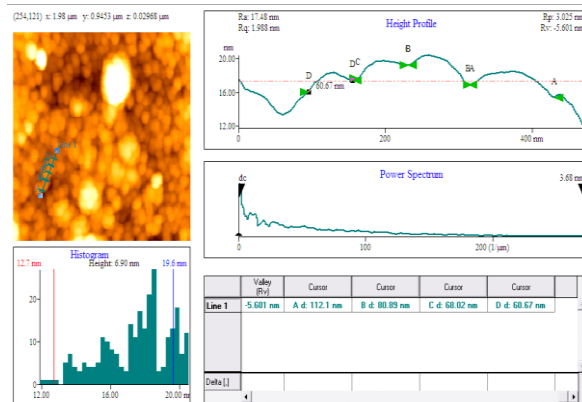


Fig (11) Reduction temperature T=200 °c for 10 min Atomic Force Microscope (AFM)

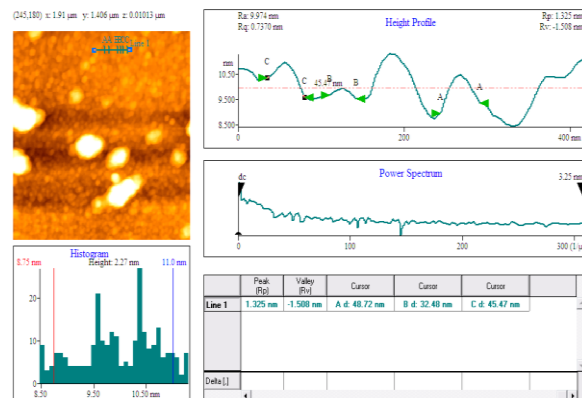


Fig (12) Reduction temperature T=200 °c for 10 min Atomic Force Microscope (AFM)

Table (1) Roughness and crystal size for samples exposed to hydrogen At different temperatures

Reduction temperature and time	R _{p-v}	R _{ms} Rough (R _q)	Average Rough (R _a)	Mean Ht	Median Ht	Surface Area
200 for 10 nm	68.33 nm	8.279 nm	5.753 nm	19.13 nm	17.67 nm	4.070 μm ²
300 for 10 nm	38.72 nm	5.155 nm	3.067 nm	9.537 nm	8.719 nm	4.029 μm ²

4 Conclusions

Vanadium Oxide films are deposited on glass and fused silica substrates by vacuum thermal evaporation technique using chemically pure V₂O₅ (99.5%) as a precursor.

The samples are Hydrogen gas in small preparation situ. All samples are examined by XRD to elucidate the crystalline structure as well as the existed phases. It is found that the pristine samples (5 layers) are amorphous while the reduced samples are deposited layer by layer sequentially up to five. The thickness of each layer is recorded by the evaporation system thickness monitor. The samples subjected to reduction process by crystalline structure as well as the existed phases. It is found that the pristine samples (5 layers) are amorphous while the reduced samples are crystalline. The immerge and evolution of different stoichiometric phases are identified at each reducing temperature.

References

- [1]O.M. Osmolovskaya, I.V. Murin, V.M. Smirnov and M.G. Osmolovsky Rev.Adv.Mater. Sci. 36 (2014) 70-74.
- [2]M. Kamalisarvestani, R.Saidur, S.Mekhilef, F.S.Javadi Renewable and Sustainable Energy Reviews 26(2013)353–364.
- [3]Jinhua Li, Ningyi Yuan, Jiansheng Xie Applied Surface Science 243 (2005) 437–442.
- [4]M. PrzeVniak-Welenc, M. AapiNski, T. Lewandowski, B. KoVcielska, L. Wicikowski, andW. Sadowski Journal of Nanomaterials Volume 2015, Article ID 418024, 8 pages.
- [5]Ramis MustafaO suzo glu n, PinarBilgic, Mustafa Yildirim, OkanDeniz Optics & Laser Technology 48 (2013) 102–109.
- [6]Yan Li, Dongping Zhang, Bo Wang, Guangxing Liang, Zhuanghao Zheng, Jingting Luo,Xingmin Cai, Ping Fan Shenzhen 518060, China.
- [7]Yueyan Liu, Juncheng Liu, Yuanbao Li, Danping Wang, Lin Ren, and Kaishun Zou, Optical Society of America.
- [8]Shrividhya Thiagarajan,a Mahalingam Thaiyanb and Ravi Ganesan,NewJ.Chem., 2015 39, 9471.
- [9]Jason Kekas, Anuj Dhawan, Praveen Gollakota, and John Muth, Vol. 928 2006 Materials Research Society.

[10]Se-Hee Lee, Hyeonsik M. Cheongb, Maeng Je Seong, Ping Liu, C. Edwin Tracy, Angelo Mascarenhas, J. Roland Pitts, Satyen K. Deb Solid State Ionics 165 (2003) 111 – 116.

[11]Jhjh-Syuan Ke, Sheng-Feng, Weng Ming-Cheng, Wu . Chi-Shen Lee.

[12]Liu JF, Wang X, Peng Q, Li YD (2005) Vanadium pentoxide nanobelts: highly selective and stable ethanol sensor materials. Adv Mater 17(6):764

[13]Liu J, Cao GZ, Yang ZG, Wang DH, Dubois D, Zhou XD, Graff GL, Pederson LR, Zhang JG (2008) Oriented nanostructures for energy conversion and storage. ChemSusChem 1(8–9):676–697

[14]M. PrzeVniak-Welenc, M. AapiNski, T. Lewandowski, B. KoVcielska, L. Wicikowski, andW. Sadowski Hindawi Publishing Corporation Journal of Nanomaterials Volume 2015, Article ID 418024, 8 pages

[15]R. Santos, J. Loureiro, A. Nogueira, E. Elangovan, J.V. Pinto, J.P. Veiga, T. Busani, E. Fortunato, R. Martins, I. Ferreira, Applied Surface Science 282 (2013) 590– 594.

[16]J.J. Yu, J. Yang, W.B. Nie, Z.H. Li, E.H. Liu, G.T. Lei, Q.Z. Xiao, A porous vanadium pentoxide nanomaterial as cathode material for rechargeable lithium batteries, Electrochimica Acta 89 (2013) 292–299.7

[17]A. Gies, B. Pecquenard, A. Benayad, H. Martinez, D. Gonbeau, H. Fuess, A. Levasseur, Effect of silver co-sputtering on V₂O₅ thin films for lithium microbatteries, Thin Solid Films 516 21 (2008) 7271–7281.

[18]M.A. Kaid, Characterization of electrochromic vanadium pentoxide thin films prepared by spray pyrolysis, Egyptian Journal of Solids 29 (2006) 273–291.